Analysis of combustion mode and operating route for hydrogen fueled scramjet engine

Article *in* International Journal of Hydrogen Energy · May 2013

DOI: 10.1016/j.ijhydene.2013.02.135

INTERNATIONAL JOURNAL OF HYDROGEN ENERGY 38 (2013) 5928–5935

Available online at www.sciencedirect.com

SciVerse ScienceDirect

journal homepage: www.elsevier.com/locate/he

Analysis of combustion mode and operating route for hydrogen fueled scramjet engine

Ruifeng Cao, Juntao Chang, Wen Bao*, Manli Guo, Jiang Qin, Daren Yu, Zhongqi Wang*

Harbin Institute of Technology, Harbin 150001, China

ARTICLE INFO

Article history:
Received 11 January 2013
Received in revised form
24 February 2013
Accepted 27 February 2013
Available online 23 March 2013

Keywords:
Performance optimization
Hydrogen fueled scramjet
Combustion mode

ABSTRACT

Hydrogen fueled scramjet is a candidate for use as the engine of the aerospace plane for its high specific impulse. To further improve the specific impulse performance, analysis of combustion mode and operating route for a hydrogen fueled scramjet engine was investigated in this study. A scramjet engine with two-staged hydrogen injection was simulated by one-dimension numeric method within the acceleration from Mach 4 to 7. Three typical combustion modes (scramjet-mode, transitional mode and ramjet-mode) could be attained by changing the total amount of fuel added or adjusting the fuel distribution between two injectors. Simulation results show that better thrust performance can be achieved as more fuel injected at the upstream fuel injector as possible, while ensuring the engine safety. From a standpoint of specific impulse maximization, an optimal scramjet combustion mode database was presented and the boundary of the combustion mode transition was determined. Meanwhile, optimal operating route was also suggested for scramjet operation in this study.

1. Introduction

Hydrogen fueled dual-mode scramjet engines can operate on a wide range of flight Mach numbers [1] and have considerable potential for trans-atmospheric vehicle applications [2,3]. Hydrogen possesses superior characteristics to any other hydrocarbon fuel in terms of ignitability, low ignition delay, and higher flame stability. These inherent advantages turn it received increased attention [4–6]. The wide range operation of scramjet engine depends on the combustion mode transitions during the ascent trajectory, in which the flow field in the combustor changes from subsonic to supersonic or vice versa. In addition, a reasonable selection of combustion mode can reduce the heat load effectively. Therefore, the combustion mode transition becomes a hot topic in current research on the scramjet engine.

One area of focus in this research was the definition and identification of the combustion modes. Sullins [7] and Mitani et al. [8] reported respectively that they observed two different combustion modes with respect to the amount of fuel. More detailed investigations were conducted by Masumoto et al. [9] and Takahashi et al. [10–12]. They distinguished four different combustion modes, namely non-ignition, weak combustion, strong combustion and thermal choking. The different combustion modes were identified on the basis of the location and brightness of the flame, the intensity of the heat flux, the shock wave systems and the pressure rise. Further research on mode transition was the transition mechanism. Chun et al. [13] expounded that the mode transitions were caused by a higher effective back pressure and resulted in changes in the shock train structures. Explanation of transition mechanism put forward by Kanda et al. [14] was based on the formation of

* *Corresponding authors*. Tel./fax: +86 0451 86403142.
E-mail addresses: changjuntao@hit.edu.cn (J. Chang), baowen@hit.edu.cn (W. Bao).
0360-3199/$ – see front matter
http://dx.doi.org/10.1016/j.ijhydene.2013.02.135

Nomenclature

A	area, m^2
C_f	friction coefficient
C_p	specific heat of mixture, kJ/(kg K)
D	equivalent diameter, m
E	total internal energy, kJ/kg
F	thrust increment of the combustor, N
$\overline{F}$	flux term
g	gravity accelerator, m^2/s
h_f	fuel combustion heat, kJ/kg
$\overline{H}$	source term
I_{sp}	specific impulse, m/s
k	specific heat ratio
L	length of combustor, m
$\dot{m}_a$	mass flow rate of air, kg/s
$\dot{m}_f$	mass flow rate of fuel, kg/s
Ma	Mach number
p	static pressure, Pa
p^*	pressure of specified unstart detection point, Pa
q	heat flux, W/m^2
Q_{lim}	limited integral value of the thermal flux, W
t	time, s
T	temperature, K
T_{lim}	limited temperature, K
$\overline{U}$	solution vector
V	velocity, m/s
x	streamwise distance from the entrance of isolator, m
$\overline{x}$	streamwise distance from the injector location, m
x_φ	length for complete mixing, m
φ	fuel equivalence ratio
σ_p	inlet unstart margin
δ_i	divergence angle of combustor, rad
η_m	combustion efficiency = mixing efficiency
ρ	density, kg/m^3

Subscripts

0	entrance conditions of isolator
e	exit conditions of combustor
ref	reference condition

the merged-recirculation region. Mitani et al. [8] focused on the upstream propagation of the combustion region in the weak mode to explain the mode transition mechanism and their viewpoint had been agreed by Kouchi et al. [15]. The latter thought that the driving force of the transition was combustion-generated high pressure.

Most of the previous studies mentioned above have been conducted in the direct-connected scramjet combustor with constant entrance conditions or/and with one-staged fuel injection. On one hand, however, throughout the flight envelope from Mach 4 to 7, the characteristic of scramjet engine changes widely in the thrust and combustion mode. So the optimal combustion mode should be employed to match the thrust command. On the other hand, it is found that there is sufficient preponderance in multi-staged fuel injection [16,17]. One benefit of multi-staged fuel injection is mitigating or avoiding the combustor–inlet interaction. Another more notable benefit is that it can increase the thrust under the limitation of peak pressure by attaining an additional pressure rise in the divergent section and broaden the engine operating range in each combustion mode. For these reasons, the analysis of combustion mode and operating route of a hydrogen fueled scramjet engine with multi-staged fuel injection is imperative and should be paid special focus to.

In the present study, the performance characteristics of scramjet engine throughout the whole flight envelope from Mach 4 to 7 were investigated and the combustion modes were analyzed and optimized for the scramjet engine with the two-staged fuel injection. For this purpose, a one-dimension numeric simulation had been conducted herein to simulate the engine performance with different flight conditions and fuel injection. In order to make the results more to be close to reality, some security restrictions for the scramjet operation, such as inlet unstart, excess temperature and excess wall thermal flux were considered. The final purpose of this study was to suggest an optimal operation mode database for the hydrogen fueled scramjet to achieve maximum engine performance during the acceleration from Mach 4 to 7.

2. Description of numerical simulation

2.1. *One-dimension analysis and performance parameter definitions*

There are a few of challenges in the numerical modeling of scramjet engine, such as fuel-air mixing, aero-thermodynamic heat dissipation, skin friction, heat addition due to combustion and the separation of the boundary layer. Compared with the multidimensional analysis approaches, the one-dimension analysis has been historically relied on heavily in the design and analysis of scramjet combustor. The analysis of heat addition to a variable area duct was originally discussed by Shapiro [1]. More recently, many scramjet combustor models with different fidelity have been constructed to support the scramjet design studies [18,19].

The governing equations for the scramjet combustor used in this study are formulated using a strategy similar to that in Ref. [20]. The equations are based on the following assumptions:

1) Quasi-one-dimensional flow (therefore, all flow variables) and the geometric area of the duct are functions of the axial distance x along the duct.
2) The flow properties are uniform across any given cross section.
3) The flow in the combustor behaves as an ideal gas with variable specific heat.
4) The aero-thermodynamic process of flow in the combustor is adiabatic process.

Due to the one-dimensional assumption, the two-dimensional Navier–Stokes equations could be reduced to a set of one-dimensional unsteady inviscid flow equations and rewritten in vector form as:

$$\frac{\partial\overline{U}}{\partial t}+\frac{\partial\overline{F}}{\partial x}=\overline{H} \tag{1}$$

where

$$\overline{U}=\begin{bmatrix}\rho A\\ \rho VA\\ \rho EA\end{bmatrix} \tag{2}$$

$$\overline{F}=\begin{bmatrix}\rho VA\\ \rho V^2+\rho A\\ \rho VHA\end{bmatrix} \tag{3}$$

$$\overline{H}=\begin{bmatrix}0\\ -\frac{\rho V^2 A}{2}\frac{4C_f}{D}+p\frac{\partial A}{\partial x}\\ h_f\frac{\partial \dot{m}_f\eta_m}{\partial x}\end{bmatrix} \tag{4}$$

$$E=\frac{p}{\rho(k-1)}+\frac{V^2}{2} \tag{5}$$

An experimental correlation in the following manner suggested in Ref. [21] is used here to calculate mixing efficiency at any streamwise distance x from the injector location:

$$\eta_m=1.01+0.176\times\ln(\overline{x}/x_\varphi), \tag{6}$$

and the length for complete mixing (x_φ) can be calculated by

$$x_\varphi/x_{\varphi\mathrm{ref}}=0.1791\times\exp\left(1.72\times\left(\varphi/\varphi_{\mathrm{ref}}\right)\right), \tag{7}$$

where the reference condition is different at each Mach number.

The skin friction [22] is found by,

$$C_f=0.0018+0.001958(\varphi\eta_m)+0.00927(\varphi\eta_m)^2+0.0088525(\varphi\eta_m)^3. \tag{8}$$

The empirical relationship [23] for the determination of the specific heat of the gas mixture model used in this study is as follows,

$$C_p=1.0575\times10^3-4.4890\times10^{-1}T+1.1407\times10^{-3}T^2-7.9999\times10^{-7}T^3+1.9327\times10^{-10}T^4. \tag{9}$$

The parameter distributions along the combustor are obtained by solving the PDEs using MacCormack's method, coupled to the models about some crucial physical effects. This method is second-order-accurate in space and time [24]. The thrust F of a scramjet combustor is calculated as the difference between the impulse function at the combustor exit and the isolator entrance (Eq. (10)). It should note that this thrust is the thrust increment produced by the combustor.

$$F=\dot{m}_a(V_e-V_0)+(p_eA_e-p_0A_0) \tag{10}$$

Hence, the specific impulse I_{sp} can be written as

$$I_{sp}=\frac{F}{\dot{m}_f g}=\frac{\dot{m}_a(V_e-V_0)+(p_eA_e-p_0A_0)}{\dot{m}_f g} \tag{11}$$

A lot of restrictions exist in the scramjet operation, such as inlet unstart, excess wall temperature and excess thermal flux through the wall. All of these abnormal modes will make the scramjet engine unsafe and should be avoided. In this numerical analysis, the operation safety boundaries about these unsafe modes were defined respectively.

Inlet unstart: the pressure ratio between the specified unstart monitoring point (p^*, 5 cm downstream from the entrance of isolator in this simulation) and the entrance of the isolator (p_0) exceed a set value σ_p (Eq. (12)).

$$\text{inlet unstart}: \frac{p^*}{p_0}\geq\sigma_p \tag{12}$$

Excess wall temperature: the maximum temperature in the combustor exceeds a limited temperature T_{lim}, which depends on the heat-resistant limit of the material (Eq. (13)).

$$\text{excess wall temperature}: \max[T(x)]\geq T_{\mathrm{lim}} \tag{13}$$

Excess wall thermal flux: the integral value of the thermal flux along the engine wall exceeds a specified value Q_{lim} (Eq. (14)).

$$\text{excess wall thermal flux}: \int_0^L q(x)dA(x)\geq Q_{\mathrm{lim}} \tag{14}$$

In the following simulation, critical values of the abnormal modes are set as $\sigma_p=1.05$, $T_{\mathrm{lim}}=2000$ K and $Q_{\mathrm{lim}}=4\times10^6$ W respectively.

2.2. *Combustor configuration and simulation conditions*

Fig. 1 presents the schematic diagram of the subscale scramjet combustor simulated in this study. The rectangular combustor, with a constant width of 100 mm, consists of a constant-area isolator and a diverging combustion chamber. Hydrogen was injected perpendicularly with sonic speed at the location of 280 mm and 580 *mm* from the entrance of the isolator. The hydrogen injection pressure is 2 MPa and the injection temperature is 300 K.

In order to meet the purpose of this study, the acceleration from flight Mach number 4 to 7 was simulated. The corresponding inflow conditions of the isolator are presented in Table 1. All these parameters are estimated based on the designed scramjet flight envelope and inlet performance analysis. For a designed flight trajectory, the flight Mach number and other flow parameters can be calculated from the flight altitude based on constant dynamic pressure flight trajectory. The dynamic pressure used in this simulation is 50,000 N/m2. The outlet parameters of the inlet (the inflow parameters shown in Table 1) are calculated using a universal

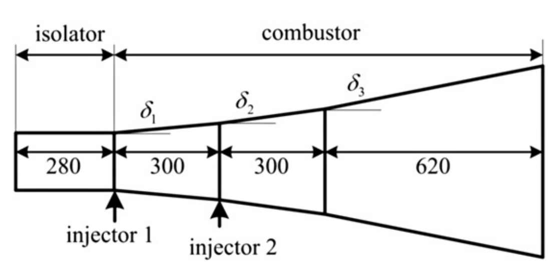

Fig. 1 – Schematic illustration of the simulated scramjet combustor.

Table 1 – Flow conditions of simulation.

Parameter	Ma 4	Ma 5	Ma 6	Ma 7
Total pressure, Pa	884,880	1,224,700	1,972,600	3,080,000
Total temperature, K	955	1269	1504	2080
Ma_0	1.5	2	2.5	3

performance analysis model recommended in the reference [25]. The inflow conditions of other flight Mach number is obtained using linear interpolation.

3. Results and discussions

3.1. *Definition of typical combustion mode*

It is ascertained that there exist some combustion modes in the scramjet engine and the mode transition should be employed during the acceleration. As described previously, various definitions and descriptions about combustion modes have been used by many researchers. With all that in mind and taking account to simulation results in this study, we suggest a definition of the three typical combustion modes: ramjet-mode, transitional mode and scramjet-mode. The profiles of Mach number and static pressure through the engine are plotted in Fig. 2 for each combustion mode which occurs during vehicle acceleration. The three combustion modes are marked by "A", "B" and "C" respectively and drawn in different shadows.

As the shadow area marked by "A" in Fig. 2, at a lower Mach number or/and at a higher total fuel equivalence ratio, a strong pre-combustion shock train occurs in the isolator and reduces the flow to subsonic. The heat addition is so strong that the flow is thermally choked at the diverging area section. We refer to this situation as the ramjet-mode. There are an adverse pressure gradient in the isolator due to the shock wave and a favorable pressure gradient in the combustor due to the separated boundary layer reattachment in the ramjet-mode.

As the vehicle accelerates, the Mach number increases, and in this so-called transitional mode the Mach number at the entrance of combustor remains supersonic. The strength of the pre-combustion shock train weakens as compared with that in the ramjet-mode, as shown in Fig. 2. There is believed to be two sonic points in the combustor because of the matching of the separated boundary layer and the heat addition. So an adverse pressure gradient occurs firstly in the upstream of the combustor and in the downstream, heat added into subsonic flow cause the static pressure to decrease. In the transitional mode the main combustion process occurs in the transonic region.

Then consider the topmost shadow areas in Fig. 2a labeled by "C". Further acceleration leads to a high Mach number and the scramjet-mode occurs. There exists no thermally choke yet in the combustor and the flow keeps supersonic along the duct in this combustion mode. Going a step further, scramjet-mode can be divided into early scramjet-mode and late scramjet-mode. In the early scramjet-mode, the boundary layer separation and pre-combustion shock train still exist, however, get thinner and weaker. So a small adverse pressure gradient exists in the upstream of the combustor. Due to the balance of the effective flow area and heat addition, nearly constant pressure combustion occurs in the midstream. In the late scramjet-mode, the disappearance of the pre-combustion shock train and boundary layer separation are the principal features.

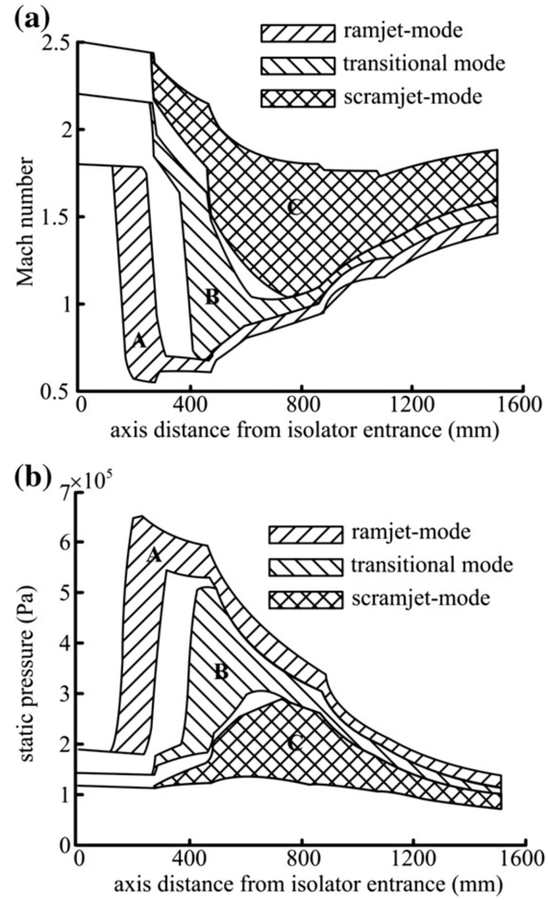

Fig. 2 – Profiles of Mach number and static pressure for three typical combustion modes of scramjet engine. The plot in this figure is based on the simulation results.

3.2. *Analyses process*

In this work, we will find the optimal combustion mode and operating route of the scramjet engine through analyzing the various factors that determine the performance of the engine. To make it easier to understand the analysis process, a brief description of the analysis step is provided before the detailed analysis.

Step 1: analyze the effect of two-staged fuel injection on the engine performance.
Step 2: analyze the effect of security restrictions on the engine performance.
Step 3: analyze the effect of flight Mach number on the engine performance.
Step 4: select the optimal realizable operating mode.

Firstly to understand the effect of two-staged fuel injection on the scramjet engine performance, we consider the case of scramjet operating at a constant Mach number of 5 and a constant altitude firstly. In this case, as shown in Fig. 3, different combustion modes could occur when the total fuel equivalence ratio or the fuel injection scheme changes.

Fig. 4 illustrates the variation of the engine thrust increment F with the proportion of fuel injection, defined by the percentage of the fuel flow injected at the upstream fuel injector. A monotonic increasing relation is found between the proportion of fuel injection and the engine thrust increment in each combustion mode. But it should note that the rate of thrust change is clearly different at various modes and there is an obvious drop in thrust at the mode transition boundary between transitional mode and ramjet-mode. This drop is mainly due to the sudden increase of total pressure loss caused by the emergence of strong pre-combustion shock train. Finally, it is found from the figure that the scramjet engine can achieve a better performance as more as possible fuel injected at the upstream fuel injector, while ensuring the engine safety. The further simulation results show that this tendency is kept at other Mach numbers.

However, as shown in Fig. 4, a lot of restrictions exist in the scramjet operation and this could easily leads to the unsafe work conditions if excess fuel injected upstream. At a lower flight Mach number, the excess fuel injected upstream tends to cause the inlet unstart; at a larger flight Mach number, it could result in the excess temperature and excess thermal flux. Hence, as shown in Fig. 5, a maximum allowable value of the proportion of fuel injection exists at a selected flight Mach number.

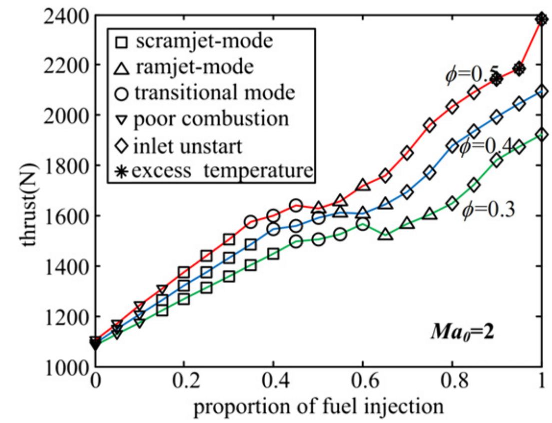

Fig. 4 – Variation of thrust with proportion of fuel injection.

Now let's focus on the effect of flight Mach number on the scramjet engine performance. Taking account into the restrictions discussed above, the realizable operating mode of the scramjet engine at different flight Mach numbers is analyzed to get the most appropriate combustion mode. Figs. 6–8 show some results of the analysis for different Mach numbers. In each figure, the horizontal axis is the total fuel equivalence ratio from 0.15 to 0.6 and the vertical axis is the engine thrust F. The unsafe operating conditions are also displayed in the figures to help understanding the analysis process of combustion mode selection. Note that there is a black solid line between the safe and unsafe operating condition in each figure. It means that the scramjet has the best performance if it works at the condition marked on the curve.

We can find from the results that for a constant flight Mach number, several possible combustion mode can be achieved either by changing the total amount of fuel added or by changing the proportion of fuel injection. Let's take the case of flight Mach number of 5 ($Ma_0 = 2.0$) shown in Fig. 7 for

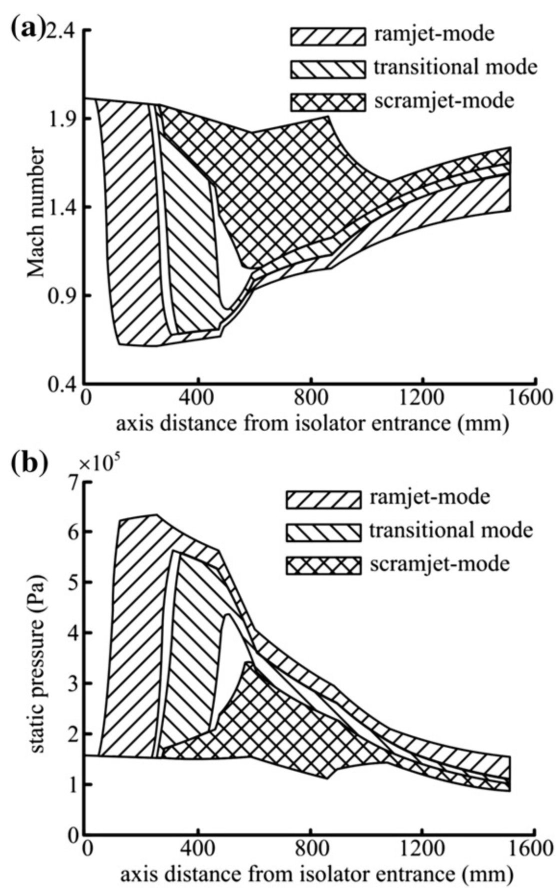

Fig. 3 – Schematic of Mach number and static pressure for constant flight Mach number of 5 and constant altitude.

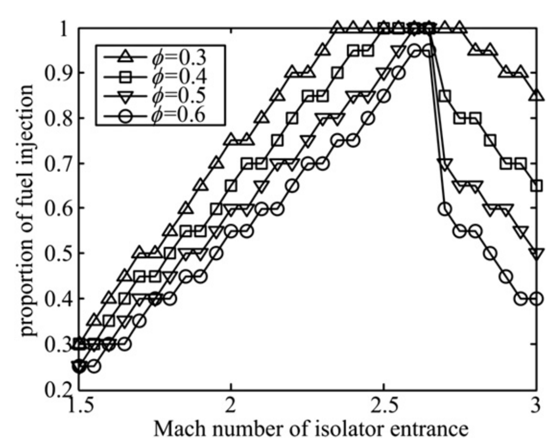

Fig. 5 – Maximum allowable value of the proportion of fuel injection vs. Mach numbers of isolator entrance.

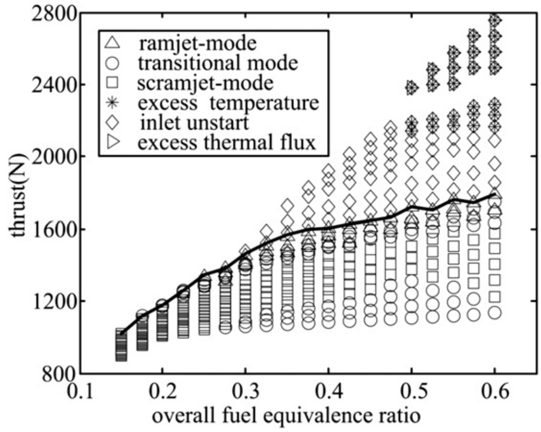

Fig. 6 – The operating mode of scramjet engine for different Mach numbers.

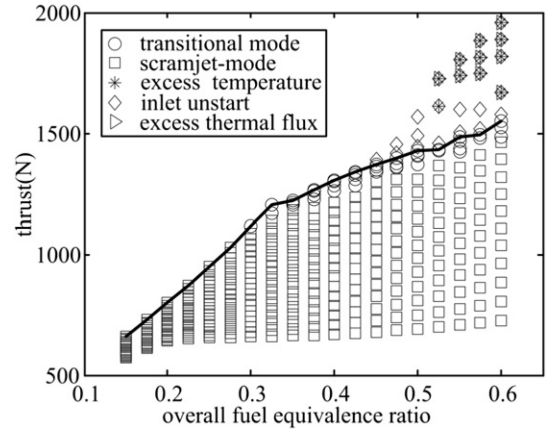

Fig. 8 – Optimal scramjet combustion and operating route.

example to analyze the mode transition characteristics in detail. The scramjet engine is in scramjet-mode when the total amount of fuel added is small. The mode transition from scramjet-mode to transitional mode and from transitional mode to ramjet-mode may occur as the fuel added is increased. For a large equivalence ratio (generally larger than 0.3), three types of combustion modes can be obtained by adjusting the proportion of the fuel injection: ramjet-mode with more fuel injected upstream, scramjet-mode with more fuel injected downstream and transitional mode with moderate fuel distribution. However, it should be pointed out particularly that if the fuel is injected too much in the downstream injector, the engine no longer operate at the scramjet-mode but transitional mode because of the intensive heat release. But less thrust is produced by the engine because the fuel-air mixing and combustion is limited in a short space in this case. This may not be a desired way in realistic operation of scramjet engine.

Taking the results shown in Figs. 6–8 together, we can found that the realizable operating mode of the engine is distinct at various flight conditions, as shown in Fig. 9. To keep the graph simple and clear, only the data of lower and upper boundary are represented here. The region of different combustion mode is rounded up approximately by different line patterns. At a low flight Mach number, the engine can operate at ramjet-mode and transitional mode. As the flight Mach number increase, the scramjet-mode can be achieved as well. When the flight Mach number is greater than 6, the scramjet-mode is almost the attainable operating mode of the scramjet engine in consideration of the performance and safe restrictions. These simulation results excellently agree with the conceptual analysis of the dual-mode scramjet.

As the point "*A*" plotted in Fig. 9, for a certain flight Mach number, a specified thrust, generally required by flight vehicle, can be achieved through operating at different combustion mode (overlap region between the combustion modes). Among these practicable combustion modes, there exists an optimal operating mode, with which the engine has the maximum specific impulse. From the analyses above we know that to maximize the engine performance, more fuel is preferred to be injected upstream, while ensuring the safety of the engine. Hence, the ramjet-mode is the preferential selection of the engine operating mode in the case like at point "*A*", and the transitional mode can be taken second place. The last option is the scramjet-mode if it comes to that.

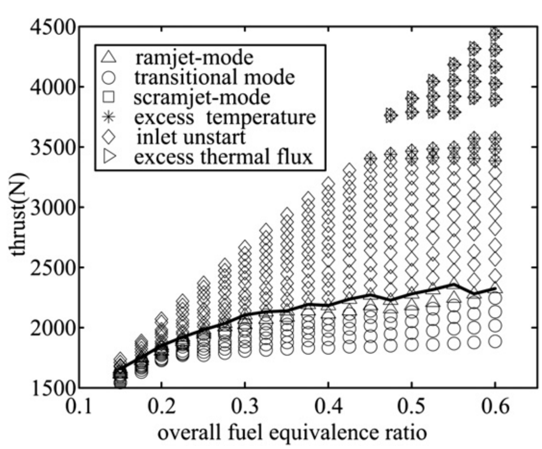

Fig. 7 – The allowable operation mode of scramjet at different Mach numbers.

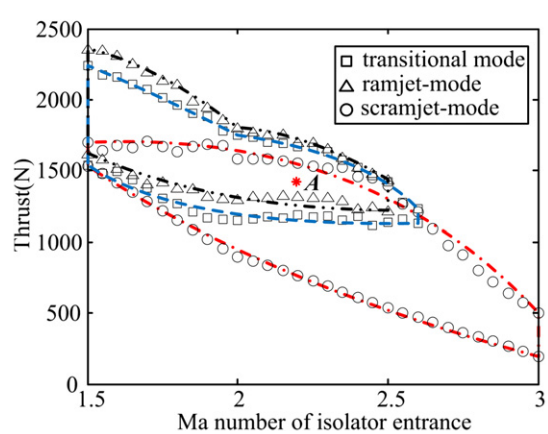

Fig. 9 – The allowable operation mode of scramjet at different Mach numbers.

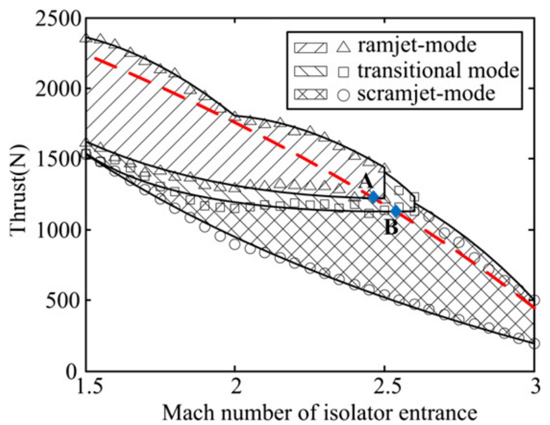

Fig. 10 – Optimal scramjet combustion and operating route.

3.3. *Analysis results*

Based on the analysis of combustion mode above, we can obtain an optimal scramjet combustion mode database as shown in Fig. 10. For the scramjet operation, the input parameters are thrust demand *F* and the flight Mach number. The output parameters are the combustion mode, the fuel equivalence ratio and the proportion of fuel injection. Hence here the optimal combustion mode database is an optimized relational table about the inputs and outputs. In this database, for a certain flight Mach number and a specified thrust *F*, the implementation of the combustion mode becomes definite and almost optimal.

To help understand the function of the optimal combustion mode database, a detail example about the application of the database is given below. In Fig. 10, the dash line represents a typical operating route of scramjet engine. The inputs and outputs of database along this operating route are shown in Table 2. The outputs of the database are the optimal inputs for the scramjet engine to achieve the specified thrust *F*.

By this time, the mode analysis and optimization for the dual-mode scramjet has been accomplished. Furthermore, the boundary of the combustion mode transition has been determined concurrently. During the typical operating route in Fig. 10, the combustion mode transition will occur on the point "A" and "B", and specific control strategy should be designed to carry out the transition and deal with the special problem accompanied in practice, for instance, the discontinuousness of the thrust.

Table 2 – A detail example about the application of the database.

Inputs of database		Outputs of database		
Ma_0	F(N)	φ	Proportion of fuel injection	Combustion mode
1.5	2250	0.48	0.3	Ramjet-mode
2	1700	0.45	0.6	Ramjet-mode
2.5	1300	0.4	1	Transitional mode
3	480	0.3	1	Scramjet-mode

4. Conclusion

A one-dimension numeric simulation method for the hydrogen fueled scramjet engine, which had a constant area isolator, followed by a divergent combustor with three different divergence angles, was used to investigate the optimization of scramjet combustion mode. The simulations were conducted within the acceleration from Mach 4 to 7 flight conditions. In these simulations, the hydrogen was injected into the combustor with two-staged fuel injection scheme, both in upstream and downstream, to examine the effect of fuel distribution on the scramjet engine performance.

By varying the total amount of fuel added or adjusting the fuel injection scheme, three typical combustion modes can be attained: scramjet-mode, transitional mode and ramjet-mode. The results show that better thrust performance can be achieved as more fuel injected at the upstream fuel injector as possible, while ensuring the engine safety.

Under some circumstances, the thrust demand can be supplied through different combustion modes. From a specific impulse maximization viewpoint, there is an optimal operating mode to meet the demanded engine thrust uniquely. Thus an optimal scramjet combustion mode database is obtained to guide the scramjet operation and meanwhile, the boundary of the combustion mode transition has been determined. The optimal operating route was also suggested for scramjet operation.

Acknowledgments

This work was supported by China National Natural Science Foundation (No. 91216105, No. 91116001, No. 51121004).

REFERENCES

[1] Heiser WH, Pratt DT. Hypersonic airbreathing propulsion. AIAA Education Series; 1993.
[2] Billig FS. Research on supersonic combustion. J Propul Power 1993;9:499–514.
[3] Cockrell CE, Auslender AH, Guy RW, McClinton CR, Welch SS. Technology roadmap for dual-mode scramjet propulsion to support space-access vision vehicle development. AIAA-2002-5188 2002.
[4] Bao W, Qin J, Zhou WX, Yu DR. Effect of cooling channel geometry on re-cooled cycle performance for hydrogen fueled scramjet. Int J Hydrogen Energy 2010;35:7002–11.
[5] Qin J, Bao W, Zhou WX, Yu DR. Flow and heat transfer characteristics in fuel cooling channels of a recooling cycle. Int J Hydrogen Energy 2010;35:10589–98.
[6] Choudhuri AR, Gollahalli SR. Combustion characteristics of hydrogen-hydrocarbon hybrid fuels. Int J Hydrogen Energy 2000;25:451–62.
[7] Sullins GA. Demonstration of mode transition in a scramjet combustor. J Propul Power 1993;9:515–20.
[8] Mitani T, Chinzei N, Kanda T. Reaction and mixing-controlled combustion in scramjet engines. J Propul Power 2001;17:308–14.

[9] Masumoto R, Tomioka S, Kudo K, Murakami A, Kato K, Yamasaki H. Experimental study on combustion modes in a supersonic combustor. J Propul Power 2011;27:346–55.
[10] Takahashi S, Yamano G, Wakai K, Tsuez M, Kono M. Self-iginition and transition to flame-holding in a rectangular scramjet combustor with a backward step. Proc Combust Inst 2000:705–12.
[11] Takahashi S, Demise S, Oshita M, Ikeda T. Correlation between heat flux distribution and combustion mode in a scramjet combustor. ISABE; 2001. 2001–1191.
[12] Takahashi S, Tanaka H, Noborio D, Miyashita T. Mach 2 supersonic combustion with hydrocarbon fuels in a rectangular scramjet combustor. ISABE; 2003. 2003–1172.
[13] Chun J, Scheuermann T, von Wolfersdorf J, Weigand B. Experimental study on combustion mode transition in a scramjet with parallel injection. AIAA-2006-8063 2006.
[14] Kanda T, Kudo K, Murakami A. Combustion with boundary layer/fuel jet interaction in a scramjet combustor. Jpn Soc Mech Eng 2000:209–14 [in Japanese].
[15] Kouchi T, Masuya G, Tomioka TMS. Mechanism and control of combustion-mode transition in a scramjet engine. J Propul Power 2012;28:106–12.
[16] Tomioka S, Murakami A, Kudo K, Mitani T. Combustion tests of a staged supersonic combustor with a strut. J Propul Power 2001;17:293–300.
[17] Thomas SR, Guy RW. Scramjet testing from Mach 4 to 20-present capability and needs for the nineties. AIAA-1990-1388 1990.
[18] Bussing TRA, Murman EM. A one-dimensional unsteady model of dual mode scramjet operation. AIAA-1983-0422 1983.
[19] Torrez SM, Scholten NA, Micka DJ, Driscoll JF, Bolender MA, Doman DB, et al. A scramjet engine model including effects of precombustion shocks and dissociation. AIAA-2008-4619 2008.
[20] Anderson Jr JD. Computational fluid dynamics: the basics with applications. New York: McGraw-Hill; 1995288–325.
[21] Diskin GS, Northam GB. Effect of scale on supersonic combustor performance. AIAA-1987-2164 1987.
[22] Orth RC, Billig FS, Grenleski SE. Measurement techniques for supersonic combustion testing. progress in aeronautics and astronautics 1974.
[23] Markell Kyle C. Exergy methods for the generic analysis and optimization of hypersonic vehicle concepts. MS thesis, Mechanical Engineering Department, Virginia Polytechnic Institute and State University; 2005.
[24] Wen B, Hong X, Tao C. Research on optimal regulating rule for scramjet control. AIAA-2006-8026 2006.
[25] Chang Juntao. Operation mode classification and control of hypersonic inlet start/unstart [D]. Harbin: Harbin Institute of Technology; 2008.